683. Design and analysis of a ducted fan UAV

Hongming Cai[1], Haisong Ang[2]
[1, 2] College of Aerospace Engineering, Nanjing University of Aeronautics and Astronautics
Yudao str. No. 29, Nanjing, Jiangsu, 210016, China
E-mail: [1]*caihongming@nuaa.edu.cn,* [2]*ahs@nuaa.edu.cn*

Abstract. The ducted fan unmanned aerial vehicle (UAV) can operate in vertical flight and horizontal flight. A new tilt-body ducted fan UAV with wings, which is capable of high-speed forward flight in wing-borne mode, is designed. Two fixed wings can provide sufficient lift of the ducted fan UAV in the high-speed wing-borne flight. The fixed geometry duct design reflects a compromise between low and high speed performance requirements of it. Computational fluid dynamics (CFD) and wind tunnel testing are used to study its aerodynamic characteristics in various modes. Momentum source items are utilized to replace two counter-rotating propellers in the numerical simulation. The results illustrate that the ducted fan MAV designed can hover, take off and land vertically. Furthermore, it has the ability to fly slowly in helicopter mode and fly rapidly in wing-borne mode and has excellent aerodynamic characteristics throughout the whole flight envelope.

Keywords: ducted fan, UAV, tilt, momentum source, wind tunnel testing, aerodynamic.

Introduction

In recent years, the request of the military for improved awareness and information-collection capability in combat situation has led to research into ducted fan VTOL UAVs, which can provide a small group of soldiers with a bird's eye view of the battlefield. This demand has led to the development of several of these vehicles, such as the AROD, Cypher [1, 2], iSTAR, GTSpy [3] and Solotrek [4]. These UAVs can be sent to a hostile territory or over the next hill to see what lies beyond and can be loaded with advanced camera and sensing device to report the accurate information back to the operator. As such, these vehicles need to be very robust and capable of operating in the common adverse weather condition [5].

The ducted-fan VTOL UAV behaves extremely complex aerodynamic characteristics, particularly in forward flight or a crosswind. Several reviews of ducted fan UAV aerodynamic analysis found in literatures are given, for example, Zhao et al. [6] used theoretical method, which is efficient but rough, to model the aerodynamics of the ducted fan UAV in preliminary design. Guerrero et al. [7] employed AVID OAV, a multidisciplinary optimization code for design and analysis of ducted fan VTOL UAVs, to predict the aerodynamic characteristics of the various components that comprise the ducted fan UAV. Its predicted data agrees well with the experimental data. Graf et al. [8] employed wind tunnel testing to study the aerodynamic characteristics of the ducted fan UAV. Zhao et al. [9] used CFD simulation to study the aerodynamic characteristics of ducted fan UAV. The propeller of the UAV was not taken into account which led to a big error.

In this paper, wind tunnel testing and CFD simulation methods are combined to analyze the aerodynamic characteristics of the ducted fan UAV. Wind tunnel testing is performed to measure the aerodynamic forces and moments applied in the ducted fan UAV. CFD simulation is used to study the flow pattern of the ducted fan UAV in detail.

The paper is organized as follows. In section 1, a new ducted fan VTOL UAV with several unique features is designed both in CAD model and manufacturing entity. In section 2, CFD simulation method is introduced to analyze the aerodynamic characteristics of the ducted fan UAV. And momentum source model (MSM) is used to simplify the realistic propeller. Section 3 is dedicated to the aerodynamic characteristics analysis of the UAV, obtained by wind tunnel

testing providing a positive feedback to the CFD simulation applicability through comparison between simulation and experiment results. Finally, some conclusion remarks are presented in Section 4.

Vehicle description

Some characteristics of the ducted fan VTOL UAV we design are presented in Table 1. As all UAVs are built by hand, the fuselage frame and fixed-wings are primarily made of carbon and balsa wood. These materials are used because they are light, strong and can be manipulated well. By miniaturization and optimization, it is small enough to be carried by one person and can accomplish surveillance and remote sensing applications in so-called 3D (dull/dirty/dangerous) environment.

Table 1. Ducted fan UAV parameters

Parameter	Value
Diameter of duct	0.13 (m)
Chord of duct	0.25 (m)
Mass	0.5 (kg)
Aspect ratio	2.0
Span of wing	0.5 (m)
Chord of wing	0.09 (m)
Weight of UAV	0.5 (kg)
Cruise speed	14 (m/s)

In order to allow the widely flight envelop, some significant design aspects of the UAV are as follows:
(1) A pair of contra-rotating propellers is installed in the middle of ducted-fuselage to provide sufficient thrust to allow the UAV hovering and taking/landing off vertically.
(2) Two fixed wings mounted on the duct rim allow good performance in horizontal flight.
(3) The fixed geometry duct design reflects a compromise between low and high speed performance requirement.
(4) Several conventional control surfaces are submerged in the propeller exhaust flow to improve control authority.
(5) The UAV can hover, take off and land vertically and fly rapidly in wing-borne mode.

Fig. 1 shows the ducted fan VTOL UAV designed in this paper. It consists of a duct, wing, fuselage, propeller, duct, tail, control surfaces and stator.
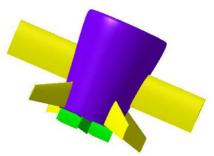

Fig. 1. The ducted fan VTOL UAV designed

Fig. 2 illustrates the definitions of the coordinate systems and respective forces and moments of the ducted fan UAV. Note that when the vehicle is in hover, the angle of attack is

90 degrees, and as the vehicle tilts into the wind, the angle of attack begins to decrease. This convention is typical of other fixed wing aircraft.
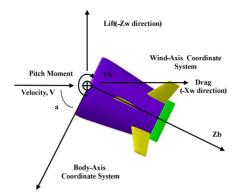

Fig. 2. CAD image of baseline model with definitions of the coordinate systems

An adverse aerodynamic force that a ducted fan UAV must deal with is the "momentum drag". Momentum drag, also referred to as "ram drag", is result of the duct changing the direction of the free-stream air, as shown in Fig. 3. The momentum drag force acts at the center of pressure of the turning airstream. The center of pressure is normally above the center of gravity of the ducted fan UAV, creating a positive pitching moment. At low speeds, the momentum drag and the resulting pitching moment are the dominant aerodynamic terms.
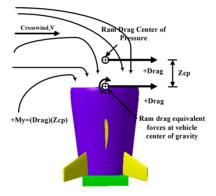

Fig. 3. Ram drag forces and moments acting at the vehicle center of gravity in a crosswind

The windward side of the duct experiences larger velocity and lower pressure than the leeward side, resulting in more lift in the windward side. The additional lift results in a positive pitching moment which reduces the ability of the ducted fan UAV to tilt into the wind and achieve forward flight. Moreover, as the UAV tilts into the wind the asymmetric flow turning into the duct causes the windward lip to experience a higher angle of attack compared to the leeward lip, further increasing the asymmetry of the aerodynamic lift distribution.

A primary consideration in the design of a ducted fan UAV is to place the center of gravity near the center of pressure to decrease the adverse pitching moment. If the distance between the center of gravity and the centre of pressure is small, the momentum drag has a small effect on the positive pitching moment.

The duct and duct lip shape are important design parameters for the ducted fan UAV. Good performance of the UAV requires a duct lip design that provides big static thrust while

702

minimizing the nose-up moments as much as possible. The fixed geometry duct design in this paper reflects a compromise between low and high speed performance requirements.

CFD simulation

CFD method

Computational fluid dynamic (CFD) methods, proposed in the early 1970's, are routinely employed in the fields of aircraft, car, and ship design. Furthermore, CFD methodologies are also applied in meteorology, oceanography, astrophysics, oil recovery and architecture. Particularly in the aeronautics industry, thanks to the rapidly increasing speed of supercomputers and due to the development of a variety of numerical acceleration techniques like multigrid and chimera grids, CFD is becoming an increasing important design tool in aircraft design and also a substantial research tool in relative research fields. According to an investigation released by AIAA indicates that 30%-50% of the aerodynamic database was provided by CFD while experimental methods such as wind tunnel and PIV just play a secondary role in aircraft design. CFD possess the capability to reduce the time cost of aircraft design and therefore proved as an efficient and low-cost tool.

Momentum source model

Precise modeling of a propeller is difficult for a variety reasons. The rotational motion of the blades with respect to the fuselage ensures that the aerodynamic problem is naturally unsteady. What's more, the low speed of the UAV makes the flow associated with propeller occurs at low Reynolds numbers. Designers need to simplify the propellers and predict the aerodynamic performance of the ducted fan UAV. The momentum source method (MSM) may be sufficient as it captures the pressure change [10, 11].

In the momentum source model, the propeller is treated as a black box, where the energy is changed within the fluid by introducing a MSM in the cylindrical region enclosing the propeller. This method has been used in previous rotor modeling studies [12, 13]. The MSM is accomplished by removing the geometry of the propeller, leaving an open passage. In its place, a momentum source is applied evenly throughout the propeller region. The momentum equation in the cylindrical region can be expressed as:

$$F_x - \frac{1}{\rho}\frac{\partial \rho}{\partial x} + v\nabla^2 u_x + \frac{v}{3}\frac{\partial}{\partial_x}d\dot{w}\overline{u} + S'_x = \frac{du_x}{dt}$$

$$F_y - \frac{1}{\rho}\frac{\partial \rho}{\partial y} + v\nabla^2 u_y + \frac{v}{3}\frac{\partial}{\partial_y}d\dot{w}\overline{u} + S'_y = \frac{du_y}{dt} \qquad (1)$$

$$F_z - \frac{1}{\rho}\frac{\partial \rho}{\partial z} + v\nabla^2 u_z + \frac{v}{3}\frac{\partial}{\partial_z}d\dot{w}\overline{u} + S'_z = \frac{du_z}{dt}$$

where the momentum source items are induced by blade element theory.

Mesh generation

Fig. 4 illustrates the computational grids around the ducted-fan UAV. The flow near the UAV induces a larger pressure gradient than the far-field. In order to obtain a high-accuracy model and reduce the computational cost, the grids should be scattered in the region where the flow changed slowly and therefore multi-blocked grids technique come into utilization. A small scaled cylinder was placed between the certain UAV and the entire computational domain.

In this paper, hexahedron grids were employed in the momentum source cylinder, which

can be used to simulate the aerodynamic characteristics of propeller. The mesh density gradually scattered from the propeller-tip (with 0.1 mm) to the propeller shaft (with 0.3 mm) and the grids in the axial direction were generated with dereference of 0.2 mm.
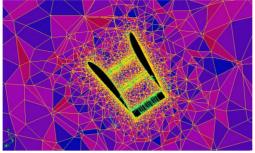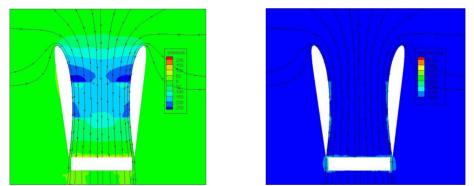

Fig. 4. Grid around the ducted fan UAV

Simulation results

Fig. 5 illustrates the sectional streamline, pressure and vortex cloud picture of the ducted fan UAV in hover at a propeller speed of 12500 rpm. The airstream turning into the duct is symmetric, which causes no ram drag and nose-up moment. The static pressure in the duct lip is very low, which leads to a large duct lift. Four tip vortexes form in the propeller tips due to pressure differences between the upper and lower wing surfaces. The tip vortexes are week due to the presence of duct, which explains the higher lift generated by ducted fan compared with isolated propeller. As shown in Fig. 5(a), the lower propeller generates a lower lift than the upper propeller due to the effects of upper propeller slipstream.
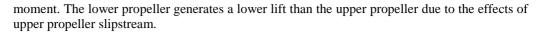

(a) Sectional streamline and pressure cloud   **(b)** Sectional streamline and vortex cloud
Fig. 5. Sectional streamline, pressure and vortex cloud picture of the ducted fan UAV in hover

As indicated in Fig. 6, the aerodynamic lift of the ducted fan UAV increases with vertical velocity at various propeller speeds. The ducted fan UAV can hover when the propeller speed is 12500 rpm. The steady vertical velocity is -7m/s at a propeller speed of 15000 rpm.

Fig. 7 shows the proportion trends of duct lift as a function of vertical velocity at various fan speeds. The duct lift proportion basically stays unchanged at different propeller speeds. The duct lift proportion decreases as the vertical velocity increases. The duct barely generates aerodynamic lift when the propeller speed is 10000 rpm and the vertical velocity is 8 m/s.

Fig. 8 illustrates the sectional streamline, pressure and vortex cloud picture of the ducted fan UAV. The duct changing the direction of incoming airstream causes a ram rag and a nose-up moment. A low static pressure zone is formed in the windward lip, which increases the nose-up
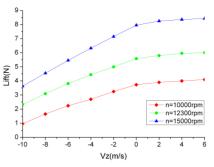
704

moment. The lower propeller generates a lower lift than the upper propeller due to the effects of upper propeller slipstream.

Fig. 6. Lift trends as a function of vertical velocity at various propeller speeds
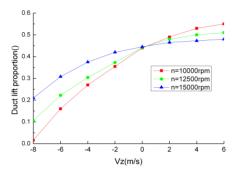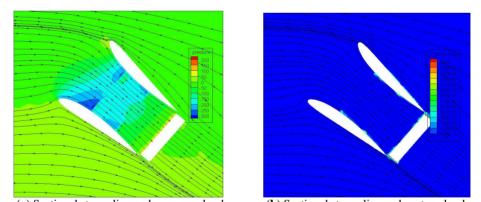

Fig. 7. Duct lift proportion trends as a function of vertical velocity at various propeller speeds

(a) Sectional streamline and pressure cloud   **(b)** Sectional streamline and vortex cloud
Fig. 8. Sectional streamline, pressure and vortex cloud picture of the ducted fan UAV in the forward flight

Fig. 9 illustrates the aerodynamic lift, drag and moment trends as a function of angle of attack at various fan speeds and forward velocities. By plotting the lift and drag together on the same plot, the reader can more efficiently determine the angle of attack necessary to maintain position (drag equal to zero). As one would expect, the UAV must tilt more into the wind as the forward velocity increases. As an example, in a forward velocity of 4 m/s (Fig. 9(a)), the ducted fan UAV must tilt into the wind approximately 60 degrees to maintain position. At 10 m/s (Fig. 9(c)), the necessary angle is approximately 70 degrees. It is interesting to note that the
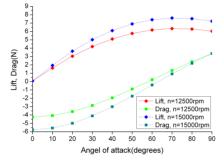
maximum lift does not occur when the thrust vector is vertical ($\alpha = 90°$). For instance, in Fig. 9(a), which shows the lift at a forward velocity of 4 m/s, the maximum lift occurs at an angle of attack of 70 degrees. This can be attributed to the duct's contribution to the lift. The fact that there is not a sudden drop in the lift after the angle of maximum lift implies that the duct lip stalls gradually. As shown in Fig. 9(b) and Fig. 9(c), the elevator has enough control authority to trim the ducted fan UAV.
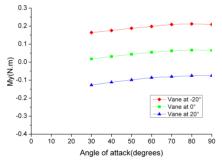
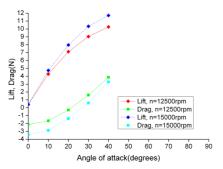## Wind tunnel testing

Wind tunnel description

The ducted fan UAV designed in this paper is small and has a low Reynolds number around 50000. The wind tunnel testing was performed in the Stability Wind Tunnel of Nanjing University of Aeronautics and Astronautics. Table 2 shows the primary technical parameters of the low Reynolds number wind tunnel.
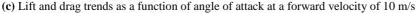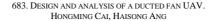
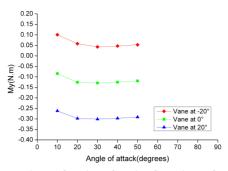**(a)** Lift and drag trends as a function of angle of attack at a forward velocity of 4 m/s

(b) Pitching moment trends as a function of angle of attack at a forward velocity of 4 m/s

(c) Lift and drag trends as a function of angle of attack at a forward velocity of 10 m/s
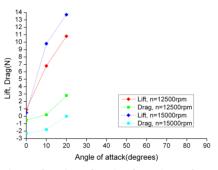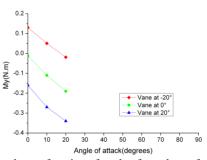
(d) Pitching moment trends as a function of angle of attack at a forward velocity of 10 m/s

(e) Lift and drag trends as a function of angle of attack at a forward velocity of 14 m/s

(f) Pitching moment trends as a function of angle of attack at a forward velocity of 14 m/s

Fig. 9. Lift, drag and moment trends as a function of angle of attack at various fan speeds and forward velocities

Table 2. Technical parameters of the wind tunnel

Technical parameter	Value
Length $\times$ width $\times$ height/ m^3	$1.7 \times 1.5 \times 1.0$
Maximum wind velocity/m	35
Minimum wind velocity/m	3
Turbulence/%	≤ 0.07
Pitch declination /°	≤ 0.5
Yaw declination /°	≤ 0.5

Fig. 10 provides the model configuration used in the wind tunnel. To position the model over the large range of pitch angels required, the model was mounted sideways. Table 3 illustrates the conditions of the wind tunnel testing.

707

Fig. 10. The ducted fan UAV in wind tunnel

Table 3. Test conditions

Parameter	Value
Wind velocity/ms-1	0, 4, 10, 14
Propeller speed/rpm	0, 10000, 12500, 15000
Angle of attack/°	0~90
Elevator angle/°	-20, -10, 0, 10, 20

Six-component sting balance

Due to the small size and low speed of the ducted fan UAV, the data accuracy of the forces and moments demands more compared with usual wind tunnel testing. A micro six-component sting balance is adopted in this paper, as shown in Fig. 11. Table 4 illustrates the micro balance parameters in wind tunnel testing.
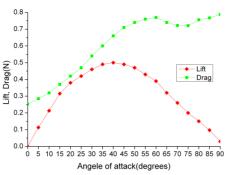

Fig. 11. Micro balance in wind tunnel testing

Table 4. Balance parameters in wind tunnel testing

Parameter	Load range	Precision/‰
Drag/N	3.136	1.08
Lift/N	9.800	1.25
Side force/N	4.900	0.99
Roll moment/(N·m)	0.1764	0.68
Yaw moment/(N·m)	0.3038	0.97
Pitch moment/(N·m)	0.4704	0.55

Experiment results

Fig. 12 illustrates the aerodynamic lift, drag and pitching moment trends as a function of angle of attack in power-off mode. The trends of lift, drag and pitching moment agree well with

reference [14]. There is no sudden drop in the lift after the angle of maximum lift, which implies a good stall characteristic.

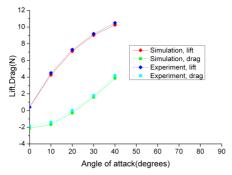**(a)** Lift and drag trends as a function of angle of attack at a tunnel velocity of 4 m/s

(b) Pitching moment trends as a function of angle of attack at a tunnel velocity of 4m/s

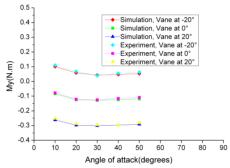**Fig. 12.** Lift, drag and pitching moment trends as a function of angle of attack

Fig. 13 illustrates the comparison of wind tunnel testing results and numerical simulation results at a forward velocity of 10 m/s. The fact that the simulation results agree well with the experiment results implies that the numerical simulation is reliable. The error can be attributed to simplification and computation precision of the numerical simulation. The manufacture error, installation error and stand interference should also be taken into account.

Conclusion

In this paper a new ducted fan VTOL UAV is designed and analyzed by numerical simulation and wind tunnel testing. The CFD simulation method is proved to be high-precision and authentic. When in hover mode, the duct lift rapidly increases with propeller speed but its proportion barely changes with propeller speed. When in vertical flight mode, the aerodynamic lift of the UAV decreases with the increasing vertical velocity, which can be attributed to the duct lift rapidly decreasing. When in forward flight mode, the ducted fan UAV needs to tilt more into the wind as the forward velocity increase. In the whole flight envelop, the elevator has enough control authority to trim and has the ability to react to further changes in environmental conditions. The ducted fan UAV designed in this paper can hover, take off and land vertically, fly slowly in helicopter mode and fly rapidly in wing-borne mode and has good aerodynamic characteristics throughout the whole flight envelope.

(a) Lift and drag trends as a function of angle of attack at a tunnel velocity of 10m/s

(b) Pitching moment trends as a function of angle of attack at a tunnel velocity of 10 m/s

Fig. 13. Lift, drag and pitching moment trends as a function of angle of attack

References

[1] **McGonigle K. P., Ferraro J., Cycon J. P.** Unmanned VTOL ground surveillance. 1994. American 5575438.

[2] **Murphy D. W., Bott J. P., Bryan W. D., et al.** MSSMP: no place to hide. Proceedings AUVSI, 1997. P. 281-290.

[3] **Johnson E. N., Turbe M. A.** Modeling, control, and flight testing of a small ducted-fan aircraft. Journal of Guidance, Control, and Dynamics, 29(4), 2006. P. 769-779.

[4] **Moshier M., Bulaga R.** Wind tunnel performance investigation of the Solotrek XFV ducted fan system. DARPA/DSO, Arlington, VA, 2001.

[5] **Will E. Graf** Effects of duct lip shaping and various control devices on the hover and forward flight performance of ducted fan UAVs. Virginia: Virginia Polytechnic Institute and State University, 2005.

[6] **Hui W. Z., Bil C.** Ducted fan VTOL UAV simulation in preliminary design. 9th AIAA Avitation Technology, Integration and Operations Conference, 2009. AIAA 2009-7097.

[7] **Guerrero I., Londenberg K.** A powered lift aerodynamic analysis for the design of ducted fan UAVs. 2nd AIAA Unmanned Unlimited Systems, Technologies and Operations. 2003. AIAA 2003-6567.

[8] **Graf W., Fleming J., Ng W.** Improving ducted fan UAV aerodynamics in forward flight. 46th AIAA Aerospace Sciences Meeting and Exhibit. 2008. AIAA 2008-430.

[9] **Hui W. Z., Bil C.** Aerodynamic design and analysis of a VTOL ducted-fan UAV. 26th AIAA Applied Aerodynamics Conference, 2008. AIAA18-21.

[10] **Nygaard T. A., Dimanlig A. C.** Application of a momentum source model to the RAH-66 Comanche FANTAIL. American Helicopter Society 4th Decennial Specialist's Conference on Aeromechanics, 2004. P. 21-23.

710

[11]   **Koskela H.** Momentum source model for CFD-simulation of nozzle duct air diffuser. Energy and Buildings, 6(13), 2004. P. 1011-1020.

[12]   **O'Brien David M., Jr.** (2006). Analysis of computational modeling techniques for complete rotorcraft configurations. Georgia Institute of Technology, 2006.

[13]   **Hariharan N., Sankar L. N.** A review of computational techniques for rotor wake modeling. AIAA 2000-0114.

[14]   **Fletcher H. S.** Experimental investigation of lift, drag, and pitching moment of five annular airfoils. 1957. NACA TN 4117.